Pergamon

Solid State Communications, Vol. 100, No. 7, pp. 487–491, 1996

0038–1098/96 $12.00+.00

PII: S0038–1098(96)00403-6

EXCITON–EXCITON INTERACTIONS IN HIGHLY EXCITED QUANTUM DOTS IN A MAGNETIC FIELD

Arkadiusz Wojs[a,b*] and Pawel Hawrylak[a]

[a]Institute for Microstructural Sciences, National Research Council of Canada, Ottawa, Canada K1A 0R6.
[b]Institute of Physics, Technical University of Wrocław, Wybrzeże Wyspiańskiego 27, 50-370 Wrocław, Poland

(*Received* 11 *June* 1996; *accepted* 28 *June* 1996 *by D.J. Lockwood*)

We study the effect of interactions of many electrons and holes on optical properties of quantum dots in a magnetic field. The degeneracies in the electronic structure of these artificial atoms lead to a remarkable dependence of the absorption/emission spectrum on density of excitons. This is explained in terms of remnants of hidden symmetries leading to coherent many-exciton states of weakly interacting excitons and bi-excitons. This is illustrated by detailed numerical results for highly excited lens-shaped InGaAs self-assembled dots. Copyright © 1996 Elsevier Science Ltd

Keywords: semiconductors, quantum dots, excitons.

Quantum dots (QD) are small quasi-two-dimensional semiconductor structures with discrete density of states and electronic shells similar to atoms [1, 2]. These "artifical atoms" can be charged either with conduction electrons, or with conduction electrons and valence band holes. The experiments and theory on electronic properties of QDs charged with electrons are progressing very rapidly [1, 3–6]. Recent experiments [9–12] aim at the creation of a dense electron–hole plasma in artificial atoms. Manipulating individual excitons in quantum dots could open up a number of applications, from exciton condensation in confined geometries, optical quantum logic gates [7], single-photonics [8], to quantum dot lasers [9]. Clearly, an understanding of interacting electrons and holes in quantum dots is needed.

We present here results of calculations of optical processes in quantum dots with strongly correlated electrons and holes. We show that the symmetries of the hamiltonian allow us to understand the numerical results in terms of the weakly interacting gas of excitons and bi-excitons. The theory is illustrated by realistic calculations carried out for lens-shaped InAs self-assembled quantum dots (SAD) [10].

The detailed numerical calculations [13] showed that in lens shaped quasi-two-dimensional SADs both electrons and valence band holes are confined by an effective parabolic potential. With the magnetic field B applied normal to the plane of the dot, the single particle spectra consist of Fock–Darwin (FD) levels $E(m,n)$ [1, 6]. The FD energies $E^e_{mn} = \Omega^e_+(n+\frac{1}{2}) + \Omega^e_-(m+\frac{1}{2})$, eigenstates $|mn\rangle$ and angular momenta $L^e_{mn} = m - n$ are those of two harmonic oscillators. The frequencies $\Omega_{+/-}$ of the two harmonic oscillators are equal at $B = 0$ and are tuned by the magnetic field [6]. The Zeeman energy is very small and can be neglected. The eigenstates are doubly degenerate due to spin σ. The valence band hole is treated in the effective mass approximation as a positively charged particle with angular momentum $L^h_{mn} = n - m$, opposite to the electron, and FD energies $E^h_{mn} = \Omega^h_+(n+\frac{1}{2}) + \Omega^h_-(m+\frac{1}{2})$ (ignoring the semiconductor gap E_G).

For special values of the magnetic field B_p such that $\Omega_+ = p\Omega_-$, the energy spectrum of electrons (holes) $E_{mn} = \Omega_-(n + pm + 1)$ is degenerate for $n + pm = t$, with t labeling electron (hole) shells and g_t the degeneracy of each shell. In the absence of a magnetic field, the degenerate shells can be labeled as $s, p, d, \ldots$. In a strong magnetic field, degeneracies are removed and electron (hole) energies $E(m)$ increase linearly with angular momentum $L = m$.

With a composite index $j = [m, n, \sigma]$ the hamiltonian of the interacting electron–hole system may be written in

* To whom correspondence should be addressed.

a compact form:

$$H = \sum_i E_i^e c_i^+ c_i + \sum_i E_i^h h_i^+ h_i - \sum_{ijkl} \langle ij|v_{eh}|kl\rangle c_i^+ h_j^+ h_k c_l + \frac{1}{2}\sum_{ijkl}\langle ij|v_{ee}|kl\rangle c_i^+ c_j^+ c_k c_l + \frac{1}{2}\sum_{ijkl}\langle ij|v_{hh}|kl\rangle h_i^+ h_j^+ h_k h_l. \quad (1)$$

The operators $c_i^+(c_i)$, $h_i^+(h_i)$ create (annihilate) the electron or valence band hole in the state $|i\rangle$ with the single-particle energy E_i. The two-body coulomb matrix elements are $\langle ij|v|kl\rangle$ for electron–electron (ee), hole–hole (hh) and electron–hole (eh) scattering, respectively [14].

The eigenstates $|\nu\rangle$ of the electron–hole system with N excitons are expanded in products of the electron and hole configurations $|\nu\rangle = (\prod_{i=1}^N c_{j_i}^+)(\prod_{i=1}^N h_{k_i}^+)|v\rangle$. A total of 30 single particle states of the dot, including spin, was used in calculations of SAD studied by Raymond *et al.* [10] The configurations are labeled by total angular momentum L_{tot} and zth component of total spin S_z^{tot}. We concentrate here on the optically active subspace of $L_{tot} = 0$ and $S_z^{tot} = 0$. A simple example of typical electronic configurations for zero magnetic field and $N = 7$ spin polarized excitons ($N = 13$ excitons when spin is included) are illustrated in the inset to Fig. 1(a). The energy levels are equally spaced, and their degeneracy increases with energy. Shells s,p,d are completely filled and a single exciton is present in shells f and g. Arrows indicate some relevant configurations with increasing kinetic energies. Due to the large confinement, the lowest kinetic energy configurations are an excellent approximation in the case of filled shells. When electrons and holes partially fill up a degenerate shell the states and energies are completely determined by their mutual interactions. The calculations for up to $N = 6$ excitons were carried out exactly and a combination of numerical diagonalization in a partially filled shell and the Hartree–Fock approximation extended calculations up to $N = 20$ excitons. The numerical results presented here can however be understood by considering the underlying many-particle symmetries hidden in the hamiltonian.

The interband optical processes in a quantum dot are completely described by the total interband polarization operators P_+^+ (P_-^-) and P_-^+ (P_+^-) which create (annihilate) electron–hole pairs with a definite spin configuration $P_+^+ = \sum_i c_{i\uparrow}^+ h_{i\downarrow}^+$ ($P_+^- = \sum_i h_{i\downarrow} c_{i\uparrow}$) by annihilating (creating) photons with a definite circular polarization. The remaining electron–hole pair spin configurations $\downarrow,\downarrow$ and $\uparrow,\uparrow$ correspond to dark excitons. The third component $P_z = \frac{1}{2}(N_\sigma^e + N_\sigma^h - N_L)$ measures a population inversion, i.e. a number of excitons $N_\sigma = N_\sigma^e = N_\sigma^h$ with definite spin σ in N_L of the single particle levels. P satisfies commutation relations of a 3D angular momentum: $[P^+,P^-] = 2P_z$, $[P_z,P^\pm] = \pm P^\pm$. The total polarization $P^2 = \frac{1}{2}(P^+P^- + P^-P^+) + P_z^2$ commutes with P^+.

We construct the states of the many electron–hole system as eigenstates of interband polarization operators (P^2,P_z). Let $|\nu\rangle$ denote the vacuum and N_L the number of orbitals: $P^2|\nu\rangle = \frac{1}{2}N_L(\frac{1}{2}N_L + 1)|\nu\rangle$ and $P_z|\nu\rangle = -\frac{1}{2}N_L$. We create *coherent many-exciton states* (CMES) $|N_\sigma\rangle$ with a definite number of exciton pairs by successive application of polarization raising operator: $|N_\sigma\rangle = (P_\sigma^+)^{N_\sigma}|\nu\rangle$. The states consisting of excitons created with different light polarization have different spin configurations and can be viewed as a product of two CMES: $|N_\downarrow,N_\uparrow\rangle = (P_-^+)^{N_\downarrow}(P_+^+)^{N_\uparrow}|\nu\rangle$.

Whether CMES are eigenstates of the system depends on the commutation relations between the hamiltonian and the polarization operators P^+:

$$[H,P^+] = \sum_i (E_i^e + E_i^h) c_i^+ h_i^+ - \sum_{ijk}\langle ij|v_{eh}|kk\rangle c_i^+ h_j^+ + \frac{1}{2}\sum_{ijkl}(\langle ij|v_{ee}|kl\rangle - \langle ik|v_{eh}|jl\rangle) \times (c_i^+ h_l^+ c_j^+ c_k - c_i^+ h_k^+ c_j^+ c_l) + \frac{1}{2}\sum_{ijkl}(\langle ij|v_{hh}|kl\rangle - \langle ik|v_{eh}|jl\rangle) \times (c_l^+ h_i^+ h_j^+ h_k - c_k^+ h_i^+ h_j^+ h_l). \quad (2)$$

The last two sums in equation (2) vanish if the interactions between electrons and holes are symmetric: $\langle ij|v_{ee}|kl\rangle = \langle ij|v_{hh}|kl\rangle = \langle ik|v_{eh}|jl\rangle$. For most quantum dots where electrons and holes are confined in the same physical area, the electron and hole interactions are very similar. For example, in the sample calculated here $v_{ee}/v_{eh} = v_{eh}/v_{hh} = 1.04$.

For almost symmetric interactions and the hamiltonian restricted to a single degenerate shell t, the commutator can be approximated as $[H_t,P^+] \approx E_X^t P^+$, where $E_X^t = E_t^e + E_t^h - \sum_{jk} g_t^{-1}\langle jj|v_{eh}|kk\rangle$ is an approximate exciton binding energy. The quantum number j ($-t \le j \le t$) denotes the angular momentum on a given shell. This commutation relation is a manifestation of hidden symmetry and $(P^+)^N|\nu\rangle$ are the multiplicative states [16–19]. The CMES of N_σ excitons are eigenstates of the shell hamiltonian with energies $E(N_\sigma) = N_\sigma E_X^t$. The same holds for states $|N_\downarrow,N_\uparrow\rangle$ created with different polarization. We conclude that excitons created in a given shell of a quantum dot with arbitrary combination of polarization of light form a mixture of coherent-many exciton states. The energy of these states is just the sum

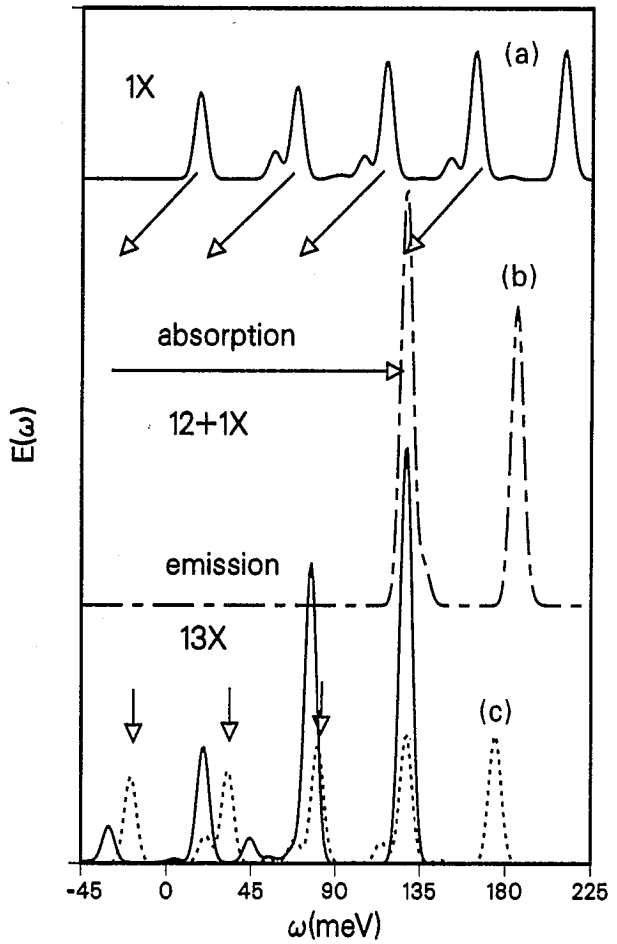

Fig. 1. Exciton addition spectrum in a quantum dot. (a) Addition spectrum of excitons into isolated individual shells (s,p,d and f) (b) addition spectrum including scattering to higher shells, empty circles correspond to the isolated shells. Inset: illustration of different configurations in the many electron–hole system.

of energies of noninteracting excitons irrespective of their spin configuration.

This assertion has been verified by exact diagonalization calculations. The CMES turned out to be excellent approximations to exact ground states with corresponding overlaps of 100% for shells s and p, and 99.8% and 99.2% for shells d and f.

In Fig. 1(a) we show the calculated addition spectrum $\mu - \mu_0$ of excitons added into independent shells of SAD [10]. Here $\mu = E_G(N) - E_G(N-1)$ is the chemical potential of the interacting system and μ_0 is the chemical potential of the noninteracting system. The shell energies are separated by $\Omega^e_+ = \Omega^e_- = 30\,\text{meV}$ for electrons and $\Omega^h_+ = \Omega^h_- = 15\,\text{meV}$ for holes. The addition energy measures the interaction energy of an added exciton with excitons already present in the dot. The lack of dependence of μ on the number of particles shows that electron–hole pairs in each independent shell form a gas of weakly interacting excitons.

Excitons begin to interact when scattering to higher energy empty shells is allowed. The scattering has a dramatic effect in rearranging spin parts of the wavefunction of CMES. This rearrangment is responsible for the formation of singlet bi-excitons. This can be understood by introducing the operator Q^+ creating singlet bi-excitons:

$$Q^+ = \frac{1}{2}\sum_{i,j}(c^+_{i\downarrow}c^+_{j\uparrow} + c^+_{j\downarrow}c^+_{i\uparrow})(h^+_{i\uparrow}h^+_{j\downarrow} + h^+_{j\uparrow}h^+_{i\downarrow}). \tag{3}$$

The bi-exciton operator satisfies a similar commutation relation as the polarization operator $[H_t, Q^+] \approx E^t_{XX}Q^+$, with $E_{XX} = 2E^t_X$. The application of Q^+ to the vacuum generates a CMES of singlet noninteracting bi-excitons. The scattering to higher shells leads to binding of bi-excitons and lowering of the bi-exciton energy $E_{XX} \to 2E^t_X - \Delta_t$ by the bi-exciton binding energy Δ_t. This is illustrated in Fig. 1(b) where we show the addition spectrum including excitations to higher shells. The main effect is a red-shift of the spectrum and a splitting of addition energies into two classes. The lower points correspond to adding bi-excitons and the upper points correspond to adding extra excitons. The splitting between the lines is the bi-exciton binding energy Δ. The numerical results show that singlet bi-excitons rather than excitons form coherent many-exciton states. The bi-exciton gas appears to be decoupled from excess excitons.

Up to now we analysed a situation of excitons in isolated shells. Now we consider the effect of filled shells. The electrons and holes in a partially filled shell interact and exchange with particles in filled shells. We can think of quasi-electrons and quasi-holes forming a gas of noniteracting bi-excitons. The formation of bi-excitons due to the scattering to higher shells is intertwinned with interaction with inter-shell charge and spin excitations. This is illustrated in the inset of Fig. 1(a). For example, the perturbative expansion of the exciton state $|\nu\rangle$ in the f-shell in the presence of filled s,p and d shells $|g\rangle$ can be written as a sum of three components [diagrams shown in the inset to Fig. 1(a)]: (a) the f-shell polarization, (b) exciton scattering to the g-shell in the presence of rigid distribution of filled shells, and (c) exciton scattering by inter-shell charge and spin excitations. It turns out that the former two mechanisms renormalize exciton energies on the scale of the bi-exciton binding energy. On the other hand, the exchange and direct contributions to the band-gap renormalization give an order of magnitude larger contribution to the addition energy, as illustrated in Fig. 2.

In the inset to Fig. 2 we summarize the evolution of the addition spectrum, including the kinetic energy, with the number of excitons N in the dot. The addition spectrum is superimposed on the the energies of peaks

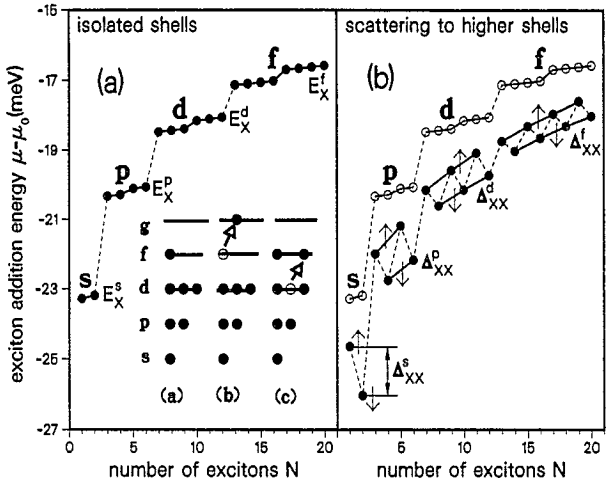

Fig. 2. Exciton addition spectrum including interaction with filled shells. Inset shows the effect of filling of the dot with excitons on the addition/subtraction spectrum.

in the absorption spectrum of a single exciton. The plateaus in the addition spectrum correspond to a gas of weakly interacting excitons and bi-excitons in partially filled shells. The spacing between plateaus and the deviations from the single exciton addition spectrum changes with increasing total number of excitons N.

In Fig. 3 we show an example of the effect of population of electrons and holes on the absorption and recombination spectrum. The upper panel shows the optical density of states (absorption spectrum) of a single exciton. We interpret each major peak as

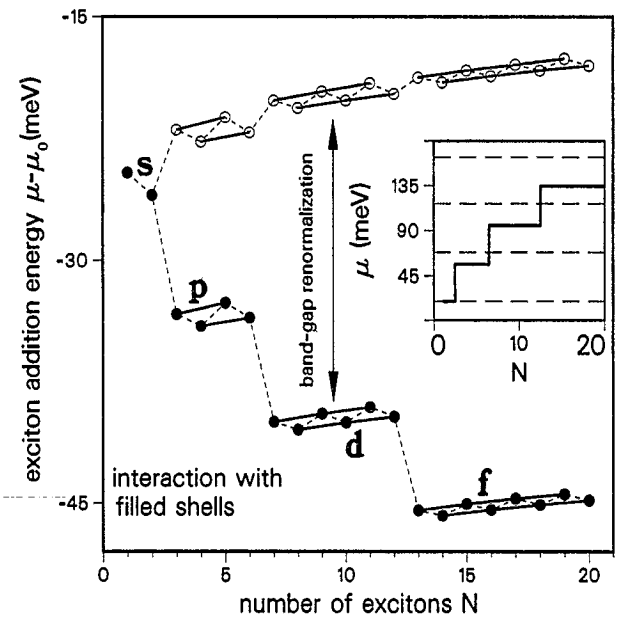

Fig. 3. Effect of many excitons on the absorption/emission spectrum. (a) Exciton absorption spectrum in empty quantum dot (b) absorption spectrum in a dot with $N = 12$ excitons (c) recombination spectrum from a dot with $N = 13$ excitons.

subtracting/adding exciton from/to a different shell of an empty QD. This spacing among peaks would be observable in, e.g. high excitation experiments on an ensemble of QDs where excitons recombine from excited states during a relaxation process, one exciton per dot at a time.

The middle panel shows the absorption spectrum for a quantum dot with $N = 12$ excitons. In an absorption process an additional exciton is created in empty f, g shells as illustrated in Fig. 1(a). The electrons and holes in filled shells block the absorption process leading to an overall blue shift of the absorption threshold. In the lowest panel we show the calculated recombination spectrum from $N = 13$ excitons. In the recombination process an exciton is removed from different shells. This creates vacancies in the electron and hole system [indicated by arrows in the inset to Fig. 1(a)]. These vacancies interact in a way excitons do. They can be interpreted as either de-excitons [19] or as charge excitations of an electron–hole droplet. The spectrum of a dense droplet of excitons consists of well separated and narrow peaks just like a density of states of a single exciton. There is however an overall red shift of the spectrum (bandgap renormalization) indicated by left pointing arrows. The spacing between peaks is also renormalized when compared with spacing of peaks in the density of states of a single exciton (shown with vertical arrows and a broken line). The spacing corresponds to charge excitations of a droplet. Hence we anticipate that the emission spectrum from highly excited QDs should reveal two different energy structures. With increasing number of excitons per dot, the single exciton spectrum would gradually be replaced by the spectrum of a weakly interacting gas of excitons in partially filled shells, and of excitations from filled to empty shells.

These conclusions are applicable for small magnetic fields and for special values of magnetic fields B_p where the shell structure is restored and the hidden symmetries operate. In the strong magnetic field limit, the hidden symmetries are completely destroyed and electrons and holes form a maximum density droplet [17].

To summarize, we have shown that strongly interacting and correlated electrons and holes in quantum dots can be understood in terms of a gas of weakly interacting excitons and bi-excitons. The chemical potential shows plateaus reflecting the shell structure of single particle energy levels. The recombination spectrum from a droplet of many excitons reflects the 0D quantized density of single particle states but the spacing is neither that of electrons and holes, nor of a single exciton, but rather reflects the excitation spectrum of the droplet.

Acknowledgements—The authors acknowledge useful discussions with S. Fafard, S. Raymond, P. Poole, S. Charbonneau, L.G. Rego, J.A. Brum, and A.H.

MacDonald. One of us (A.W.) acknowledges financial support by the Institute for Microstructural Sciences, NRC Canada.

REFERENCES

1. For recent reviews and references see: Kastner, M., *Physics Today*, p. 24, January 1993; Chakraborty, T., *Comments in Cond. Matter Phys.* **16,** 1992, 35.
2. Petroff, P.M. and Denbaars, S., *Superlattices and Microstructures* **15,** 1994, 15.
3. Hansen, W. *et al.*, *Phys. Rev. Lett.* **62,** 1989, 2168.
4. Ashoori, R.C. *et al.*, *Phys. Rev. Lett.* **71,** 1993, 613.
5. Drexler, H. *et al.*, *Phys. Rev. Lett.* **73,** 1994, 2252.
6. Hawrylak, P., *Phys. Rev. Lett.* **71,** 1993, 3347.
7. For a review see Bennett, C.H., *Physics Today*, pp. 24–30 October 1995; Monroe, C. *et al.*, *Phys. Rev. Lett.* **75,** 1995, 4714.
8. Imamoglu, A. and Ymamoto, Y., *Phys. Rev. Lett.* **72,** 1994, 210.
9. Grundmann, M. *et al.*, *Phys. Status. Solidi* **188,** 1995, 249.
10. Raymond, S. *et al.* (to be published); Fafard, S. *et al.*, *Phys. Rev.* **B52,** 1995, 5752.
11. Bockelmann, U. *et al.*, *Solid State Electronics* (in press).
12. Bayer, M. *et al.*, *Phys. Rev. Lett.* **74,** 1995, 3439.
13. Wojs, A., Hawrylak, P., Fafard, S. and Jacak, L., *Phys. Rev. B* (in press).
14. Wojs, A. and Hawrylak, P., *Phys. Rev.* **B51,** 1995, 10 880.
15. Lockwood, D.J. and Young, J.F. (eds), *Light Scattering in Semiconductor Structures and Superlattices.* pp. 479–490. NATO ASI273, Plenum, 1991.
16. Lerner, I.V. and Lozovik, Yu.E., *Zh. Eksp. Teor. Fiz.* **80,** 1981, 1488 [*Sov. Phys. JETP* **53,** 1981, 763].
17. Paquet, D., Rice, T.M. and Ueda, K., *Phys. Rev.* **B32,** 1985, 5208.
18. MacDonald, A.H. and Rezayi, E.H., *Phys. Rev.* **B42,** 1990, 3224.
19. Bychkov, Yu.A. and Rashba, E.I., *Phys. Rev.* **B44,** 1991, 6212.